JPET # 265686

Title Page

Adrenoceptor responses in human embryonic stem cell-derived cardiomyocytes: A special focus on electrophysiological property

Weiwei Jiang[2#], Xingjian Hu[1#], Fei Li[1], Geng Li[1], Yin Wang[1,3*]

[1]Department of Cardiovascular Surgery, Union Hospital, Tongji Medical College, Huazhong University of Science and Technology, Wuhan, China

[2]Department of Gastroenterology, Union Hospital, Tongji Medical College, Huazhong University of Science and Technology, Wuhan, China

[3]Department of Biomedical Engineering, The Johns Hopkins University, Baltimore, MD, United States

[#]These authors contributed equally to the work.

Running Title: Electrophysiological response of hESC-CMs to AR stimulation

Recommended section assignment: Cardiovascular

***Correspondence**: Yin Wang, Department of Cardiovascular Surgery, Union Hospital, Tongji Medical College, Huazhong University of Science and Technology, 1277 Jiefang Ave, Wuhan, Hubei, 430022, China. E-mail address: wangyin0817@hotmail.com

The number of text pages: 33

Number of tables: 1

Number of figures: 8

Number of references: 34

Number of words in the Abstract: 250

Number of words in the Introduction: 289

Number of words in the Discussion: 1383

List of abbreviations:

CMs: cardiomyocytes; hESCs: human embryonic stem cells; AR: adrenergic receptor; CV: conduction velocity; hESC-CMs: human embryonic stem cell-derived cardiomyocytes; hPSC-CMs: human pluripotent stem cell-derived cardiomyocytes; AP: action potential; APDs: action potential durations

Abstract

Human embryonic stem cell-derived cardiomyocytes (hESC-CMs) have become a promising cell source for cardiovascular research. The electrophysiological characteristic of hESC-CMs has been generally studied, but little is known about electrophysiological response to adrenergic adrenoreceptor (AR) activation. This study aims to characterize electrophysiological response of hESC-CMs to adrenergic stimulation, in terms of the conduction velocity (CV) and action potential (AP) shape. The H9 hESC-CMs were acquired by a classical differentiation protocol and cultured to achieve confluent cell monolayers. The AP shape and CV among the monolayers were recorded using optical mapping during electrophysiological and pharmacological stimulation experiments. RT-qPCR and Western blot were adopted to determine the expression levels of connexin and ion channel gene and protein. Chronic β-AR stimulation by isoproterenol for 24h in hESC-CMs monolayers increased CV by approximately 50%, while α-AR or acute β-AR stimulation had no significant effect; Chronic β-AR stimulation resulted in a significant Cx43 and $Na_{v1.5}$ up-regulation at both protein and mRNA level. Isoproterenol induced CV accelerating and Cx43, $Na_{v1.5}$ up-regulation in hESC-CMs, which was attenuated by selective β1-adrenoceptor antagonist CGP-20712A, but not selective β2-antagonist ICI-118551. Moreover, pretreatment with PKA inhibitor H89, MEK inhibitor SB203580 and MAPK inhibitor PD98059 suppressed the isoproterenol-induced CV accelerating and Cx43 up-regulation, whereas had no significant effect on $Na_{v1.5}$ up-regulation. The AP shape in hESC-CMs monolayers was less susceptible by either β-AR or α-AR stimulation. It is β1-AR, not β2-AR contributing to the modification of conduction velocity among hESC-CMs monolayers. Chronic β1-AR stimulation accelerates CV by up-regulating Cx43 via PKA/MEK/MAPK pathway.

Statement of Significance

These provide new insight into the electrophysiologic characteristics of human embryonic stem cell-derived cardiomyocytes(hESC-CMs) and depict a concise signaling pathway in the ARs regulation of action potential shape and electrical propagation across hESCs-CMs monolayer. It is β1-AR, not β2-AR contributing to the modification of conduction velocity in hESC-CMs and accelerates conduction velocity by up-regulating Cx43 via PKA/MEK/MAPK pathway.

Introduction

Human pluripotent stem cell-derived cardiomyocytes (hPSC-CMs), including induced pluripotent and embryonic stem cell-derived cardiomyocytes (hiPSC-CMs and hESC-CMs, respectively), has become an important cell resource for cardiac regeneration, drug screening, and model of cardiovascular disease. (Dakhore et al., 2018; Protze et al., 2019; Samak and Hinkel, 2019). One particularly crucial for the usages of hPSC-CMs is an profound understanding of their electrophysiological property (Liu et al., 2016). The electrophysiologic characteristics of hPSC-CMs have been investigated by several studies, mostly of which focused on the properties of specific ion transporters, including sodium current (I_{Na}), calcium current (I_{Ca}), potassium current(I_k) and so on, whereas the relationship between adrenergic receptor (AR) signaling and electrophysiologic characteristics of hPSC-CMs, has not yet been revealed (van den Heuvel et al., 2014; Wang et al., 2019).

As a canonical signaling pathway for the cardiomyocyte, the stimulation of AR system increases beating rate, force of contraction and velocity of contraction/relaxation in adult cardiomyocytes (Campbell et al., 2014). While attention has been given primarily to the regulatory mechanisms of AR signaling on the beating rate and contractility, few studies explored the effect of AR signaling on the electrophysiological characters and electrical propagation among hPSC-CMs (Brito-Martins et al., 2008; Pillekamp et al., 2012). Little is known about electrophysiological response of hPSC-CMs to adrenergic adrenoreceptor (AR) and the effect of AR activation on action potential (AP) and conduction velocity (CV) is unclear. (Veeraraghavan et al., 2014).

Thus, the present study aims to (a) culture hESC-CMs to achieve confluent monolayers and perform electrophysiological and pharmacological studies using optical mapping method, (b) evaluate the alteration in APDs and average CV among the hESC-CMs monolayer following α- or β-AR stimulation, and (c) identify the possible adrenoceptor receptor subtype(s) and mechanisms involved in this process.

Methods

hESCs culture and differentiation

We cultured H9 human embryonic stem cells (hESCs) in a monolayer-based protocol (Bhattacharya et al., 2014). To be short, undifferentiated hESCs were cultured in Geltrex (Thermofisher Scientific, Waltham, MA)-coated tissue culture plates and incubated in E8 media (Thermofisher Scientific) for 4 days before differentiation. Then, the cells were incubated in RPMI 1640 (Thermofisher Scientific) with B27 without insulin (Thermofisher Scientific) to begin the differentiation. Media was supplemented with 6μM CHIR99021 (Selleckchem, Houston, TX) for the first 48 hours, then 5μM IWR-1 (Sigma-Aldrich, St. Louis, MO) for the following 48 hours. The media was then replaced with RPMI 1640 with B27 and insulin (Thermofisher Scientific) on day 9 of the differentiation. hESC-CMs monolayers were harvested using 0.05% trypsin between 10-12 days of the differentiation and re-plated at a density of 250,000 cells/cm^2 to form a confluent monolayer, which be cultured for extra 30 days (day 40-45 post-differentiation) for the experiments.

Pharmacological experiments

Targets were first dissolved with either ddH_2O or DMSO as the stock solution and then diluted to certain concentration with Tyrode's solution as the working solution. Isoproterenol (ISO, Sigma-Aldrich) dissolved in ddH_2O to 1 mM was used as the stock solution and then diluted to 1 μM in Tyrode's solution when used. CGP 20712A (Tocris, Minneapolis, MN) was dissolved in ddH_2O to 1mM as the stock solution and diluted to 0.3 μM in Tyrode's solution when used. Epinephrine (Sigma-Aldrich) was dissolved with DMSO to 10mM and diluted to 10μM in Tyrode's solution. ICI 118551 (Tocris) was also dissolved in DMSO at 10 μM as the stock solution and serially diluted to 50nM as the working solution. H89 (Sigma) was dissolved in DMSO at 1M as the stock solution and serially diluted to 10 mM as the working solution. SB203580 (Tocris) was dissolved in DMSO at 1 mM as the stock solution and diluted to 20μM as the working solution. PD98059 (Tocris) was dissolved in DMSO at 1 mM as the stock solution and diluted to 20 μM as the working solution.

Chronic adrenergic stimulation on the hESC-CMs monolayers was performed by supplementation of 1 μmol isoproterenol or 10 μmol/L epinephrine to the medium 24h before the experiments. Acute adrenergic stimulation was performed by supplementation of 1 μmol isoproterenol or 10 μmol/L epinephrine 10mins before the experiments. For some experiments, the specific inhibitors were added 1h prior to chronic stimulation with ISO.

Electrophysiological experiments

Optical mapping: hESC-CMs monolayers (250,000 cells/cm^2) were first incubated in Tyrode's solution and stained with voltage-sensitive dye di-4-ANEPPS (10 μM) (Sigma-Aldrich, St. Louis, MO) for 10 min on a 35 mm Petri dish. To eliminate cell motion and contraction

interference, an 10μM blebbistatin (Sigma-Aldrich) was applied. Point pacing was proceeded at least 10 minutes after blebbistatin was added. The experiments was conducted in a temperature controlled at 37 °C and a 100x100 pixel CMOS camera (MiCAM Ultima-L, SciMedia, Costa Mesa, CA) was used for optical action potentials recording .

Customized MATLAB scripts were used for mapping data analysis. A 5×5 Gaussian filter were applied during optical recordings to remove excessively noisy background or low-signal channels. Activation maps were drawn according to the time of maximum AP upstroke rate. CV, AP duration at 30% and 80% were calculated from the optical voltage signal.

Western Blot analysis

hESC-CMs were harvested and lysed with RIPA buffer (Thermofisher Scientific) cocktail supplemented with protease inhibitor (Sigma-Aldrich) and phosphatase inhibitor (Sigma-Aldrich). Total protein was quantified with a Pierce BCA kit (Thermofisher Scientific). A total protein lysate of 30μg were loaded for each lane on 4-12% mini Tris-Bis gels (Bio-Rad, Hercules, CA) and transferred onto PVDF membranes for immuno-blotting. Membranes were blocked with nonfat milk and then incubated with primary antibodies for Kv11.1 (Santa Cruz, 1:200, sc-377388), Kv7.1 (Santa Cruz, 1:1000, sc-20816), Nav1.5 (Alomone Labs, 1:200, asc-005), Connexin 43 (Sigma, 1:1000, C6219) and GAPDH (EMD Millipor,1:1000, MAB374) overnight at 4 °C. The membrane was further incubated with secondary antibodies (LI-COR 1:20000, goat anti-rabbit or mouse, Lincoln, NE) and imaged by Odyssey CLX (LI-COR) per the manufacturer's protocol. Detailed information of the antibodies was shown in Table 1. ImageJ software was used for a quantified and normalized protein intensities analysis.

Quantitative RT-PCR

Quantitative RT-PCR was performed on hESC-CMs monolayers after mRNA was extracted as routine. Reverse transcription was performed to create cDNA with the PCR Master Mix kit (Thermo Fisher Scientific), using the MyGo Mini PCR system (IT-IS Life Science Ltd., Republic of Ireland). RT-qPCR was performed on each target in triplicate. Primer sequence of the PCR products were listed below: GJA1-sense, ACAGGTCTGAGTGCCTGAAC and GJA1-antisense, CGAAAGGCAGACTGCTCATC; SCN5A-sense, GTGCCCAGAAGCAGGATGAG, SCN5A-antisense, GGACATACAAGGCGTTGGTG; CACAN1C- sense, CACGGCTTCCTCGAATCTTG, CACAN1C-antisense, CTGTGGAGATGGTCGCATTG; KCNQ1-sense, CCGCCTGAACCGAGTAGAAG, KCNQ1-antisense, GTGTTGCTGGGCAGGAAGAG.

Statistical Methods

Data are presented as mean ± standard error of mean (S.E.M.). Data was analyzed with Prism 7.0 (GraphPad Software, Inc.). Student's unpaired two-tailed t test was used for two-group comparisons, and one-way ANOVA followed by Tukey's post hoc tests was conducted for multiple comparisons. $P<0.05$ was considered statistically significant.

Result

β-AR stimulation on conduction velocity (CV) and action potentials (APs) in hESC-CMs monolayers

After been point-stimulated at different pacing rates, the action potentials and their propagation across hESC-CMs monolayers were recorded using optical mapping. As shown in Fig 1A and B, the CV was faster in hESC-CMs monolayers stimulated with 1 μmol ISO for 24h, when compared with the control monolayers (11.2±0.3 cm/s vs. 7.8±0.4 cm/s at 1 Hz, $P<0.001$), the same results were observed in the other two different pacing rates (0.5 and 2 Hz). Next, we investigated the impact of chronic β-adrenergic receptor stimulation on action potentials in hESC-CMs monolayers, Fig 1C shows the recorded APs in control and chronic ISO treatment monolayers at standard 1Hz pacing rate. As shown in Fig 1D, these two groups had similar APD_{80}, but APD_{30} became longer, and repolarization rate (reciprocal of triangulation) became faster after chronic ISO treatment.

To determine whether the increasing in CV by chronic β-adrenergic receptor stimulation was associated with a regulation on the transcriptional or translational level, we compared the mRNA and protein expression of specific molecules between control and chronic ISO treatment hESC-CMs. As shown in Fig 2A, we measured the mRNA expression using RT-qPCR, and GJA1, SCN5A and CANAN1C expressions of hESC-CMs were significantly increased after stimulation with 1 μmol ISO for 24 h. In the protein level, Fig 2B and 2C show the Connexin 43 and Nav1.5 protein contents were higher in hESC-CMs with chronic ISO treatment, whereas Kv11.1(subunit of IKr channel) and Kv7.1(subunit of IKs channel) level did not differ between control and chronic ISO treatment hESC-CMs.

Next, we evaluated the effect of acute β-AR stimulation on CV and APs in hESC-CMs monolayers by treatment of the monolayers with 1 μmol ISO for 30min. As shown in Fig 3A and B, no significant difference of CV was observed before and after acute ISO treatment (8.4±0.5

cm/s vs. 8.7±0.6 cm/s at 1 Hz, *P*=0.677). Meanwhile, the action potentials of these two groups at 1 Hz pacing rate are similar, which are illustrated in Fig 3C and 3D.

α-AR stimulation on CV and APs in hESC-CMs monolayers

In order to confirm whether the observed AR effects on CV and AP appeared exclusively under β-AR stimulation, analog experiments were performed with hESC-CMs monolayers treated with 10 μmol/L PE for 24 h as chronic treatments and 30 mins as acute ones. In contrast to ISO, PE has no significant effect in altering CV. As shown in Fig 4A and B, there were no significant difference of CV among chronic α-AR stimulation, acute α-AR stimulation and control groups (8.8±0.4 cm/s vs. 8.7±0.6 cm/s vs. 9.3±0.4 cm/s at 1 Hz, *P*=0.899 and 0.311). Furthermore, upon acute α-AR stimulation, no alterations were detected in action potentials, but chronic α-AR stimulation shortens the APD_{30} (263±21 ms vs. 214±40 ms, *P*=0.049) and increases the APD triangulation (145±6 ms vs. 161±10 ms, *P*=0.015)(Fig 4C and D).

β1-AR but not β2-AR subtype involved in CV regulation in hESC-CMs

To further clarify which subtype of β-AR is responsible for the CV and APs changes, hESC-CMs monolayers were pretreated with selective β1-AR inhibitor CGP 20712A (0.3 μmol/L) or β2-AR inhibitor ICI 118551(50 nmol/L) before stimulation with ISO. The working concentration of these two inhibitors was according to published literatures(Hakuno et al., 2002; Chakir et al., 2003). As shown in Fig 5A, the increase of CV after ISO admission was significantly attenuated in the presence of CGP 20712A (10.8±0.2 cm/s vs. 8.3±0.4 cm/s, *P*=0.001), but not in the presence of ICI 118551 (10.8±0.2 cm/s vs. 10.3±0.3 cm/s, *P*=0.145) (Fig 5B). Consistent with the previous

results, chronic ISO treatment made APD_{30} longer and AP triangle lower, but only CGP 20712A attenuated these effects. (Fig 5C, D).

To further characterize how β1-AR and β2-AR involved in respond to modulation of CV and APs in hESC-CMs monolayers we examined the gene expression profiles of GJA1, SCN5A, Kv11.1 and CANAN1C. 24 h ISO treatment increased the expression of GJA1, SCN5A and CANAN1C which were consistent with the previous results. Interestingly, the up-regulation of GJA1 and SCN5A by chronic β-AR stimulation was only abolished by pre-incubation with CGP 20712A (Fig 6A). At the protein level, the results were similar with the gene level, ISO increased Cx43 and Nav1.5 expression. While pre-exposure to CGP 20712A had no effect (Fig 6B).

β-AR stimulation increasing CV of hESC-CMs by up-regulation of Cx43 expression via the PKA-MEK-MAPK pathway

To further investigate the potential mechanism and signal pathway of ISO-induced CV increasing, hESC-CMs monolayers were incubated with ISO alone or pretreated respectively with 10 mmol/L H89 (specific inhibitor of PKA), or 20 μmol/L SB203580 (specific inhibitor of MAPK), or 20 μmol/L PD98059 (specific inhibitor of MEK) for 1 h before ISO admission as previously described. As shown in Fig 7A and B, co-administration of H89/SB203580/PD98059 with ISO all could attenuate the effect to increase CV by β-AR stimulation. In addition, the APs change caused by β-AR stimulation was also suppressed by these three specific inhibitors (Fig 7C), the prolongation of APD_{30} and acceleration of repolarization rate by ISO was restained in the presence of H89, SB203580 or PD98059(Fig 7D). Again, β-AR stimulation or inhibition had little effect on APD_{80}. Importantly, inhibition of PKA-MEK-MAPK signaling prevented the

increased expression of Cx43 by ISO (Fig 8A) but have no effect on expression of Nav1.5 (Fig. 8B), suggesting PKA-MEK-MAPK pathway activated by β-AR stimulation only contribute to the regulation of Cx43 expression.

Discussion

Human embryonic stem cells derived cardiomyocytes(hESC-CMs) have emerged as the prototypical source for applications in disease modeling and drug screening differentiation(Pal, 2009; Vidarsson et al., 2010). However, such applications require hESC-CMs faithfully recapitulate the physiology of authentic adult cells, especially the electrophysiological properties(Liu et al., 2016). Previous studies of authentic cardiomyocytes revealed that adrenergic receptors (ARs) play a critical role in the regulation of the electrophysiological performance of cardiomyocytes such as the conduction velocity and the action potential(Campbell et al., 2014). In this study, we investigated the regulation effect of ARs in hESC-CMs' electrophysiological characters and demonstrated that (1) β-AR stimulation in hESC-CMs monolayers for 24h increased CV by approximately 50%, which did not occur after α-ARs stimulation; (2) β1-ARs, not β2-ARs were involved in the modulation of CV in hESC-CMs monolayers; (3) β1-AR stimulation induced marked alterations in the expression of Connexins 43 and SCN5A, which fits well with the increased CV(4)β1-AR stimulation up-regulated Cx43 expression via PKA-MEK-MAPK pathway.

The gap junction protein Connexins play an important role in regulation of CV(Campbell et al., 2014). In human heart, the main isoforms of Connexins expressed are Cx43, Cx40, Cx37 and Cx45, while Cx43 is the most abundant one(Manring et al., 2018). Radioactive labelling tests had

demonstrated that half-life of Cx43 is only 1–2h, which allows dynamic regulation of its expression and further affect the CV(Leithe and Rivedal, 2007). Considerable evidences proved that connexin expression could be altered by β-AR stimulation in animal models and primary cardiomyocytes. In adult rats, 24h continuous stimulation with isoprenaline infusion in vivo resulted in an upregulation of cardiac Cx43 expression while Cx40 remained unchanged(Salameh et al., 2006). Increases in CV (~25%) and Cx43 expression in response to 24h incubation with isoprenaline were observed in neonatal rat cardiac myocytes (NRCMs)(de Boer et al., 2007). Changes in expression of Cx43 only occurred after long exposures to isoprenaline, while some studies reported no CV increase to acute β-AR stimulation(Salameh and Dhein, 2011). In the present study, we found CV among hESC-CMs monolayers could be increased by ~50% after 24h incubation with isoprenaline, while no response was observed when exposure to isoprenaline for 10min. Moreover, the western blot and RT-qPCR analysis confirmed that expression of Cx43 and GJA1 gene was increased by ~1.5 times and ~1.8 times after chronic β-AR stimulation, respectively.

To further understand the role of different β-AR subtypes on Cx43 expression and CV regulation, the hESC-CMs were pretreatment with selective β1 or β2-AR inhibitor. We found the effect of isoprenaline on CV was only antagonized by β1-AR inhibitor, not β2-AR inhibitor. This is inconsistent with the results of a previous study, which suggested β2-AR mediates the up-regulation of Cx43-NP in NRCMs(Xia et al., 2009). One important issue need clarified is whether β2-AR been well expressed in the hESC-CMs with d40-45 post-differentiation, since the expression level of ARs has been proved to depend on the culture time. A literature confirmed that β-AR regulate beating rate and contractile responses in hESC-CMs with d29 to d79 after

differentiation, and both β1- and β2-AR gene has been detected by qRT–PCR. Moreover, the researchers found the increased beating rate after isoprenaline treatment was significantly reduced in the presence of β2-AR inhibitor(Brito-Martins et al., 2008). This can be interpreted as β2-AR existed in hESC-CMs during this period. Therefore, it is reasonable to assume that β2-AR was expressed in hESC-CMs with d40-45 post-differentiation but did not participate in the CV regulation.

Cx43 can be phosphorylated by PKA, PKC, PKG and MAPK(Marquez-Rosado et al., 2012). β1-ARs can activate adenylyl cyclase to product cAMP(Fu et al., 2014). As the direct substrate of cAMP, PKA has been implicated in the various biological responses of β1-ARs(Saad et al., 2018). Our study demonstrated that effect of β1-AR on increasing CV and regulating Cx43 expression was driven via PKA/MEK/MAPK pathway in hESC-CMs, as H89-PKA inhibitor, SB203580-MAPK inhibitor and PD98059-MEK inhibitor could attenuate the above-mentioned effect. Consistent with it, several studies have shown that activation of the cAMP/PKA pathway can regulate Cx43 expression and a downstream activation of MEK and MAPK was in dependence on PKA following isoprenaline in adult rats(Zhang et al., 2005). or in neonatal rat cardiomyocyte(Krishnamurthy et al., 2007).

The other factor which plays a role in modulation of CV is the upstroke of the AP(Perry and Illsley, 1986). The sodium channels contribute to the AP upstroke, while the magnitude of sodium currents (I_{Na}) can be increased by β-AR activation(Frohnwieser et al., 1997; Lu et al., 1999). Another study demonstrated the expression of $Na_{v1.5}$ is upregulated via CaMKII activation after β-AR stimulation(Jost et al., 2005). Therefore, the effects of β-AR on the AP upstroke are a combination of its effects on increasing the magnitude of I_{Na} and up-regulating sodium channel

expression. However, some studies indicated the predicted maximal effect of I_{Na} on CV is an increase of only 4–5% following β-AR stimulation(Boyle et al., 2019). Nevertheless, we believed the sodium channel was not the main determinant in modulation of CV by β-AR stimulation in hESC-CMs. Although optical action potentials used in our experiment could not provide direct measurements of individual sodium currents or AP upstroke, the western blot and qRT-PCR analysis confirmed that expression of Nav1.5 and SCN5A increased ~1.5X and ~2× times after chronic β-AR stimulation.

β-AR signaling also influences AP duration. The slowly activating delayed rectifier potassium channel (I_{Ks}) can be affected by β-AR stimulation via PKA pathway(Jost et al., 2007). In the present, we observed a significant prolongation of ADP_{30} in hESC-CMs after β-AR stimulation, which is discordant with the findings of other prior studies. In large mammals, β-AR stimulation increases the magnitude of I_{Ks} to promote APD shortening(Jost et al., 2005); while addition of isoproterenol can increase the steepness of the AP trace and reduces the effective refractory period in the whole hearts(Ng et al., 2007). The difference of APD change in hESC-CMs by β-AR stimulation is maybe due to the dynamic change of major repolarization potassium channels across different stages of differentiation, which was systematically characterized in our prior study, at this phase the expression of IKs is at a low level and contributes little to APD(Wang et al., 2019).

In heart failure, changes in β-AR amount and subtypes can lessen the effect of adrenergic regulation on sodium channels and Connexin proteins and attenuate the increase in conduction velocity by β-AR stimulation, which may contribute to arrhythmias(Spadari et al., 2018). The practical application of human stem cell derived- cardiomyocytes for myocardial Regeneration requires a thorough and clear understanding of the adrenoceptor response in order to reduce

their pro-arrhythmogenic potential. To our knowledge, this is the first research to systematically evaluate the electrophysiological response in hESC-CMs by β-AR and α-AR stimulation, in terms of action potential duration and conduction velocity. These findings may rich the knowledge of hESC-CMs' electrophysiological characteristics.

The study has some limitations. Firstly, we did not conduct the experiments in multiple cell lines subjected to its complexity and lengthy time span. We adopted hESCs to derive cardiomyocyte since it has been documented as the gold standard in terms of their pluripotency and natural development. Among different hESC lines, H9 line has been shown to have good cardiomyogenic potential(Sepac et al., 2012). Secondly, our study did not detect the ARs expression density and investigate the ARs response in hESC-CMs of different differentiation stages. Notably, the expression and response of ARs might be associated with the differentiation stage. Thirdly, we used the optical mapping to perform the experiments in single confluent cell monolayer and it has the advantage of hundreds of measurements from very large populations of cell, however, it cannot assess individual ionic currents and dV/dt, but it has the advantage of hundreds of measurements from very large populations of cell from in a single confluent cell monolayer, in which the cells are not affected by patch pipette solution and their structure remains unperturbed, and can measure net ionic current activity through measurements of the action potential(Herron et al., 2012). Fourthly, we use total protein western blots rather than isolated membrane ones in our study, which may affect the quantity of the results.

In conclusion, our findings confirm electrophysiological response to AR activation in hESCs-CMs and depict a concise signaling pathway in the ARs regulation of electrical propagation. It is

β1-AR, not β2-AR contributing to the up-regulation of Cx43 and modification of conduction velocity via PKA-MEK-MAPK pathway.

Authorship contributions:

Participated in research design: W. J and Y. W

Conducted experiments: W. J, X. H, F. L, G. L

Contributed new reagents or analytic tools: W. J, X. H

Performed data analysis: W. J, F. L

Wrote or contributed to the writing of the manuscript: W. J, X. H and Y. W

References

Bhattacharya S, Burridge PW, Kropp EM, Chuppa SL, Kwok WM, Wu JC, Boheler KR and Gundry RL (2014) High efficiency differentiation of human pluripotent stem cells to cardiomyocytes and characterization by flow cytometry. *J Vis Exp*:52010.

Boyle PM, Franceschi WH, Constantin M, Hawks C, Desplantez T, Trayanova NA and Vigmond EJ (2019) New insights on the cardiac safety factor: Unraveling the relationship between conduction velocity and robustness of propagation. *J Mol Cell Cardiol* **128**:117-128.

Brito-Martins M, Harding SE and Ali NN (2008) beta(1)- and beta(2)-adrenoceptor responses in cardiomyocytes derived from human embryonic stem cells: comparison with failing and non-failing adult human heart. *Br J Pharmacol* **153**:751-759.

Campbell AS, Johnstone SR, Baillie GS and Smith G (2014) beta-Adrenergic modulation of myocardial conduction velocity: Connexins vs. sodium current. *J Mol Cell Cardiol* **77**:147-154.

Chakir K, Xiang Y, Yang D, Zhang SJ, Cheng H, Kobilka BK and Xiao RP (2003) The third intracellular loop and the carboxyl terminus of beta2-adrenergic receptor confer spontaneous activity of the receptor. *Mol Pharmacol* **64**:1048-1058.

Dakhore S, Nayer B and Hasegawa K (2018) Human Pluripotent Stem Cell Culture: Current Status, Challenges, and Advancement. *Stem Cells Int* **2018**:7396905.

de Boer TP, van Rijen HV, Van der Heyden MA, Kok B, Opthof T, Vos MA, Jongsma HJ, de Bakker JM and van Veen TA (2007) Beta-, not alpha-adrenergic stimulation enhances conduction velocity in cultures of neonatal cardiomyocytes. *Circ J* **71**:973-981.

Fu Q, Kim S, Soto D, De Arcangelis V, DiPilato L, Liu S, Xu B, Shi Q, Zhang J and Xiang YK (2014) A long lasting beta1 adrenergic receptor stimulation of cAMP/protein kinase A (PKA) signal in cardiac myocytes. *J Biol Chem* **289**:14771-14781.

Hakuno D, Fukuda K, Makino S, Konishi F, Tomita Y, Manabe T, Suzuki Y, Umezawa A and Ogawa S (2002) Bone marrow-derived regenerated cardiomyocytes (CMG Cells) express functional adrenergic and muscarinic receptors. *Circulation* **105**:380-386.

Herron TJ, Lee P and Jalife J (2012) Optical imaging of voltage and calcium in cardiac cells & tissues. *Circ Res* **110**:609-623.

Jost N, Papp JG and Varro A (2007) Slow delayed rectifier potassium current (IKs) and the repolarization reserve. *Ann Noninvasive Electrocardiol* **12**:64-78.

Jost N, Virag L, Bitay M, Takacs J, Lengyel C, Biliczki P, Nagy Z, Bogats G, Lathrop DA, Papp JG and Varro A (2005) Restricting excessive cardiac action potential and QT prolongation: a vital role for IKs in human ventricular muscle. *Circulation* **112**:1392-1399.

Krishnamurthy P, Subramanian V, Singh M and Singh K (2007) Beta1 integrins modulate beta-adrenergic receptor-stimulated cardiac myocyte apoptosis and myocardial remodeling. *Hypertension* **49**:865-872.

Leithe E and Rivedal E (2007) Ubiquitination of gap junction proteins. *J Membr Biol* **217**:43-51.

Liu J, Laksman Z and Backx PH (2016) The electrophysiological development of cardiomyocytes. *Adv Drug Deliv Rev* **96**:253-273.

Manring HR, Dorn LE, Ex-Willey A, Accornero F and Ackermann MA (2018) At the heart of inter- and intracellular signaling: the intercalated disc. *Biophys Rev* **10**:961-971.

Marquez-Rosado L, Solan JL, Dunn CA, Norris RP and Lampe PD (2012) Connexin43 phosphorylation in brain, cardiac, endothelial and epithelial tissues. *Biochim Biophys Acta* **1818**:1985-1992.

Ng GA, Brack KE, Patel VH and Coote JH (2007) Autonomic modulation of electrical restitution, alternans and ventricular fibrillation initiation in the isolated heart. *Cardiovasc Res* **73**:750-760.

Pal R (2009) Embryonic stem (ES) cell-derived cardiomyocytes: a good candidate for cell therapy applications. *Cell Biol Int* **33**:325-336.

Perry RS and Illsley SS (1986) Basic cardiac electrophysiology and mechanisms of antiarrhythmic agents. *Am J Hosp Pharm* **43**:957-974.

Pillekamp F, Haustein M, Khalil M, Emmelheinz M, Nazzal R, Adelmann R, Nguemo F, Rubenchyk O, Pfannkuche K, Matzkies M, Reppel M, Bloch W, Brockmeier K and Hescheler J (2012) Contractile properties of early human embryonic stem cell-derived cardiomyocytes: beta-adrenergic stimulation induces positive chronotropy and lusitropy but not inotropy. *Stem Cells Dev* **21**:2111-2121.

Protze SI, Lee JH and Keller GM (2019) Human Pluripotent Stem Cell-Derived Cardiovascular Cells: From Developmental Biology to Therapeutic Applications. *Cell Stem Cell* **25**:311-327.

Saad NS, Elnakish MT, Ahmed AAE and Janssen PML (2018) Protein Kinase A as a Promising Target for Heart Failure Drug Development. *Arch Med Res* **49**:530-537.

Salameh A and Dhein S (2011) Adrenergic control of cardiac gap junction function and expression. *Naunyn Schmiedebergs Arch Pharmacol* **383**:331-346.

Salameh A, Frenzel C, Boldt A, Rassler B, Glawe I, Schulte J, Muhlberg K, Zimmer HG, Pfeiffer D and Dhein S (2006) Subchronic alpha- and beta-adrenergic regulation of cardiac gap junction protein expression. *FASEB J* **20**:365-367.

Samak M and Hinkel R (2019) Stem Cells in Cardiovascular Medicine: Historical Overview and Future Prospects. *Cells* **8**.

Sepac A, Si-Tayeb K, Sedlic F, Barrett S, Canfield S, Duncan SA, Bosnjak ZJ and Lough JW (2012) Comparison of cardiomyogenic potential among human ESC and iPSC lines. *Cell Transplant* **21**:2523-2530.

Spadari RC, Cavadas C, de Carvalho A, Ortolani D, de Moura AL and Vassalo PF (2018) Role of Beta-adrenergic Receptors and Sirtuin Signaling in the Heart During Aging, Heart Failure, and Adaptation to Stress. *Cell Mol Neurobiol* **38**:109-120.

van den Heuvel NH, van Veen TA, Lim B and Jonsson MK (2014) Lessons from the heart: mirroring electrophysiological characteristics during cardiac development to in vitro differentiation of stem cell derived cardiomyocytes. *J Mol Cell Cardiol* **67**:12-25.

Veeraraghavan R, Gourdie RG and Poelzing S (2014) Mechanisms of cardiac conduction: a history of revisions. *Am J Physiol Heart Circ Physiol* **306**:H619-627.

Vidarsson H, Hyllner J and Sartipy P (2010) Differentiation of human embryonic stem cells to cardiomyocytes for in vitro and in vivo applications. *Stem Cell Rev Rep* **6**:108-120.

Wang Y, Zhu R and Tung L (2019) Contribution of potassium channels to action potential repolarization of human embryonic stem cell-derived cardiomyocytes. *Br J Pharmacol* **176**:2780-2794.

Xia Y, Gong KZ, Xu M, Zhang YY, Guo JH, Song Y and Zhang P (2009) Regulation of gap-junction protein connexin 43 by beta-adrenergic receptor stimulation in rat cardiomyocytes. *Acta Pharmacol Sin* **30**:928-934.

Zhang GX, Kimura S, Nishiyama A, Shokoji T, Rahman M, Yao L, Nagai Y, Fujisawa Y, Miyatake A and Abe Y (2005) Cardiac oxidative stress in acute and chronic isoproterenol-infused rats. *Cardiovasc Res* **65**:230-238.

Footnotes

Funding

This study was financially supported by Natural Science Foundation of China (NO.81700317, NO.81400290 and NO.81670351).

Figure Legend

FIGURE 1 Comparison of electrophysiological properties of H9 hESC-CM monolayers before and after chronic β-adrenergic stimulation. (A) Representative activation map. (B) Average conduction velocity at pacing rate between 0.5,1 and 2 Hz, n=10, two-tailed unpaired t-test, **P* < .05, significantly different as indicated. (C) Action potential traces for 1 Hz pacing. (D) APD distribution of the monolayers paced at 1 Hz, n=10, two-tailed unpaired t-test, **P* < .05, significantly different as indicated. Abbreviations: APD_{30}, action potential duration at 30% repolarization; APD_{80}, action potential duration at 80% repolarization; AP triang, time from APD_{30} to APD_{80}; CV, conduction velocity.

FIGURE 2 Comparison of channel and junction proteins expression of hESC-CM monolayers with and without chronic β-adrenergic stimulation. (A) GJA1, SCN5A, CACAN1C and KCNQ1 gene expressions normalized to GAPDH, n=8 for each gene, two-tailed unpaired t-test, **P* < .05, significantly different as indicated; (B) Nav1.5, Connexin43, Kv11.1, Kv7.1 and GAPDH protein expressions; (C) Relative protein(Nav1.5, Connexin43, Kv11.1, Kv7.1) expressions normalized to GAPDH, n=6 for each protein, two-tailed unpaired t-test, **P* < .05,significantly different as indicated.

FIGURE 3 Comparison of electrophysiological properties of H9 hESC-CM monolayers before and after acute β-adrenergic stimulation. (A) Representative activation map. (B) Average conduction velocity at 1 Hz pacing rate, n=6, two-tailed unpaired t-test, *P < .05, significantly different as indicated. (C) Action potential traces for 1 Hz pacing. (D) APD distribution of the monolayers paced at 1 Hz, n=6, two-tailed unpaired t-test, **P* < .05, significantly different as

indicated. Abbreviations: APD_{30}, action potential duration at 30% repolarization; APD_{80}, action potential duration at 80% repolarization; AP triang, time from APD_{30} to APD_{80}; CV, conduction velocity.

FIGURE 4 Comparison of electrophysiological properties of H9 hESC-CM monolayers before and after acute or chronicα-AR Stimulation. (A) Representative activation map. (B) Average conduction velocity at 1 Hz pacing rate, n=6 for each group, one-way ANOVA followed by Tukey's post hoc tests, *P < .05, significantly different as indicated. (C) Action potential traces for 1 Hz pacing. (D) APD distribution of the monolayers paced at 1 Hz, n=6 for each group, one-way ANOVA followed by Tukey's post hoc tests, *P < .05, significantly different as indicated. Abbreviations: APD_{30}, action potential duration at 30% repolarization; APD_{80}, action potential duration at 80% repolarization; AP triang, time from APD_{30} to APD_{80}; CV, conduction velocity.

FIGURE 5 Comparison of electrophysiological properties of H9 hESC-CM monolayers between control, Isoproterenol, Isoproterenol+CGP-20712A and Isoproterenol+ICI 118,551 groups. (A) Representative activation map. (B) Average conduction velocity at 1 Hz pacing rate, n=6 for each group, one-way ANOVA followed by Tukey's post hoc tests, *P < .05, significantly different as indicated. (C) Action potential traces for 1 Hz pacing. (D) APD distribution of the monolayers paced at 1 Hz, n=6 for each group, one-way ANOVA followed by Tukey's post hoc tests, *P < .05, significantly different as indicated. Abbreviations: APD_{30}, action potential duration at 30% repolarization; APD_{80}, action potential duration at 80% repolarization; AP triang, time from APD_{30} to APD_{80}; CV, conduction velocity.

FIGURE 6 Comparison of channel and junction proteins expression of hESC-CM monolayers between control, Isoproterenol, Isoproterenol+CGP-20712A and Isoproterenol+ICI 118,551 groups. (A) GJA1, SCN5A, CACAN1C and KCNQ1 gene expressions normalized to GAPDH, n=8 for each gene, one-way ANOVA followed by Tukey's post hoc tests, **P* < .05, significantly different as indicated; (B) Nav1.5 and Connexin43 protein expressions normalized to GAPDH, n=5 for Nav1.5 and n=6 for Connexin43, one-way ANOVA followed by Tukey's post hoc tests, **P* < .05, significantly different as indicated.

FIGURE 7 Comparison of electrophysiological properties of H9 hESC-CM monolayers between control, Isoproterenol, Isoproterenol+H89, Isoproterenol+SB203580 and Isoproterenol+PD98059 groups. (A) Representative activation map. (B) Average conduction velocity at 1 Hz pacing rate, n=6 for each group, one-way ANOVA followed by Tukey's post hoc tests, **P* < .05, significantly different as indicated. (C) Action potential traces under 1 Hz pacing. (D) APD distribution of the monolayers paced at 1 Hz, n=6 for each group, one-way ANOVA followed by Tukey's post hoc tests, **P* < .05, significantly different as indicated. Abbreviations: APD_{30}, action potential duration at 30% repolarization; APD_{80}, action potential duration at 80% repolarization.

FIGURE8 Comparison of channel and junction proteins expression of hESC-CM monolayers between control, Isoproterenol, Isoproterenol+H89, Isoproterenol+SB203580 and Isoproterenol+PD98059groups. (A) Connexin43 expressions normalized to GAPDH, n=6, one-way ANOVA followed by Tukey's post hoc tests, **P* < .05, significantly different as indicated;

(B) Nav1.5 expressions normalized to GAPDH, n=5, one-way ANOVA followed by Tukey's post hoc tests, $*P < .05$, significantly different as indicated.

JPET Fast Forward. Published on March 26, 2020 as DOI: 10.1124/jpet.120.265686
This article has not been copyedited and formatted. The final version may differ from this version.

Table 1 Summary of antibodies used in the study

Antibody name	Commercial source	Cat#	species	epitope	isotype	RRID	Diluting buffer	Dilution
Connexin 43	Sigma-Aldrich	C6219	rabbit polyclonal	amino acid residues 363-382 of connexin 43	IgG	AB_476857	5% milk	1:1000
Nav1.5	Alomone Labs	asc-005	rabbit polyclonal	amino acid residues 17/19 of SCN5A	IgG	AB_2040001	5% milk	1:200
Kv11.1	Santa Cruz	sc-377388	mouse monoclonal	amino acid 96-120 of HERG	IgG1	none	5% milk	1:200
Kv7.1	Santa Cruz	sc-20816	rabbit polyclonal	amino acid 547-676 of KCNQ1	IgG	AB_2131551	5% milk	1:1000
GAPDH	EMD Millipore	MAB374	mouse monoclonal	Glyceraldehyde-3-phosphate dehydrogenase from rabbit muscle	IgG1	AB_2107445	5% milk	1:500
IRDye® 800CW Goat anti-Mouse IgG	LI-COR	925-32210	goat	IgG	IgG	none	5% milk	1:10000
IRDye® 800CW Goat anti-Rabbit IgG	LI-COR	925-32211	goat	IgG	IgG	none	5% milk	1:10000
IRDye® 680RD Goat anti-Mouse IgG	LI-COR	925-68070	goat	IgG	IgG	none	5% milk	1:10000
IRDye® 680RD Goat anti-Rabbit IgG	LI-COR	925-68071	goat	IgG	IgG	none	5% milk	1:10000

JPET Fast Forward. Published on March 26, 2020 as DOI: 10.1124/jpet.120.265686
This article has not been copyedited and formatted. The final version may differ from this version.

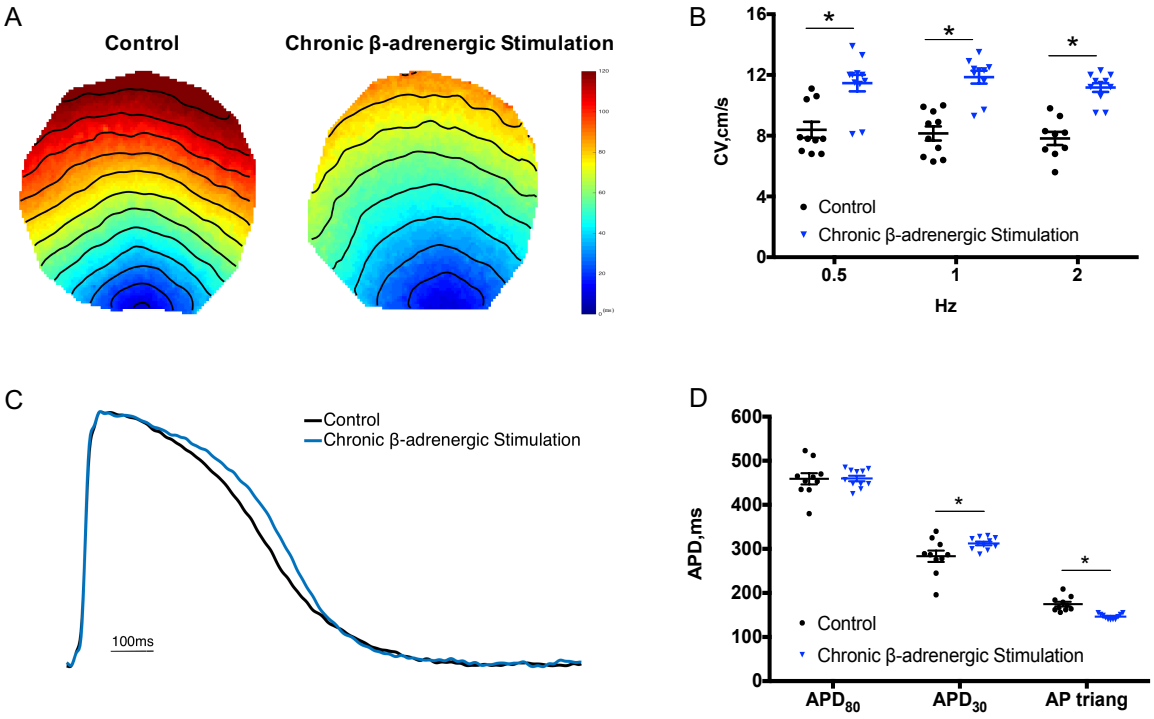

FIGURE 1

JPET Fast Forward. Published on March 26, 2020 as DOI: 10.1124/jpet.120.265686
This article has not been copyedited and formatted. The final version may differ from this version.

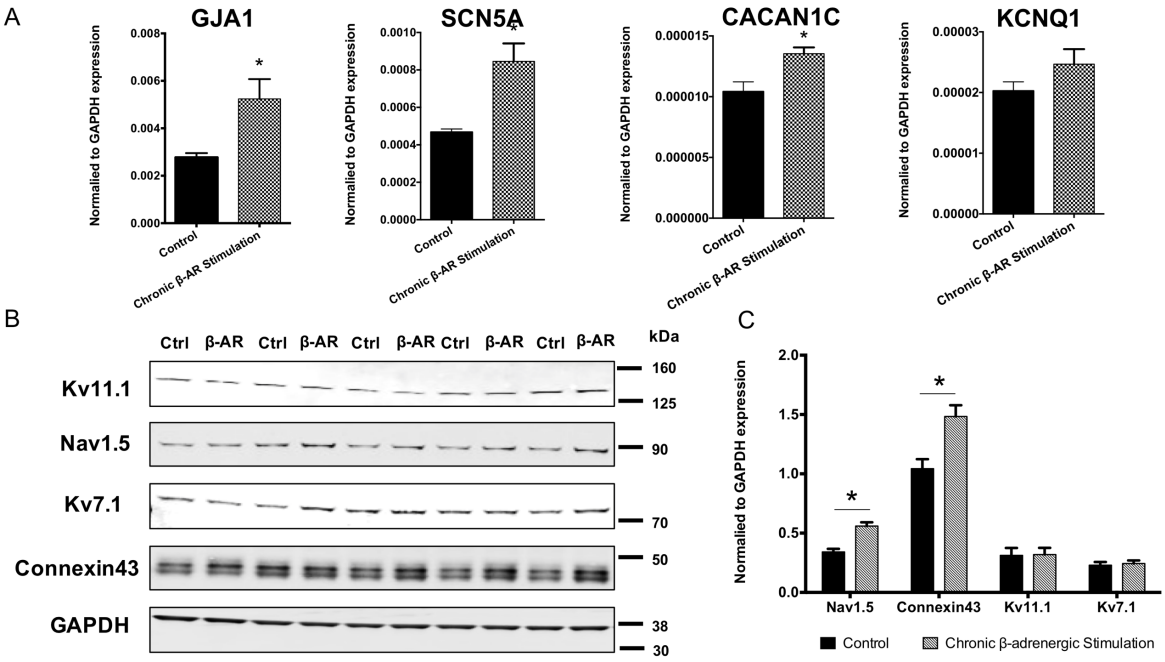

FIGURE 2

JPET Fast Forward. Published on March 26, 2020 as DOI: 10.1124/jpet.120.265686
This article has not been copyedited and formatted. The final version may differ from this version.

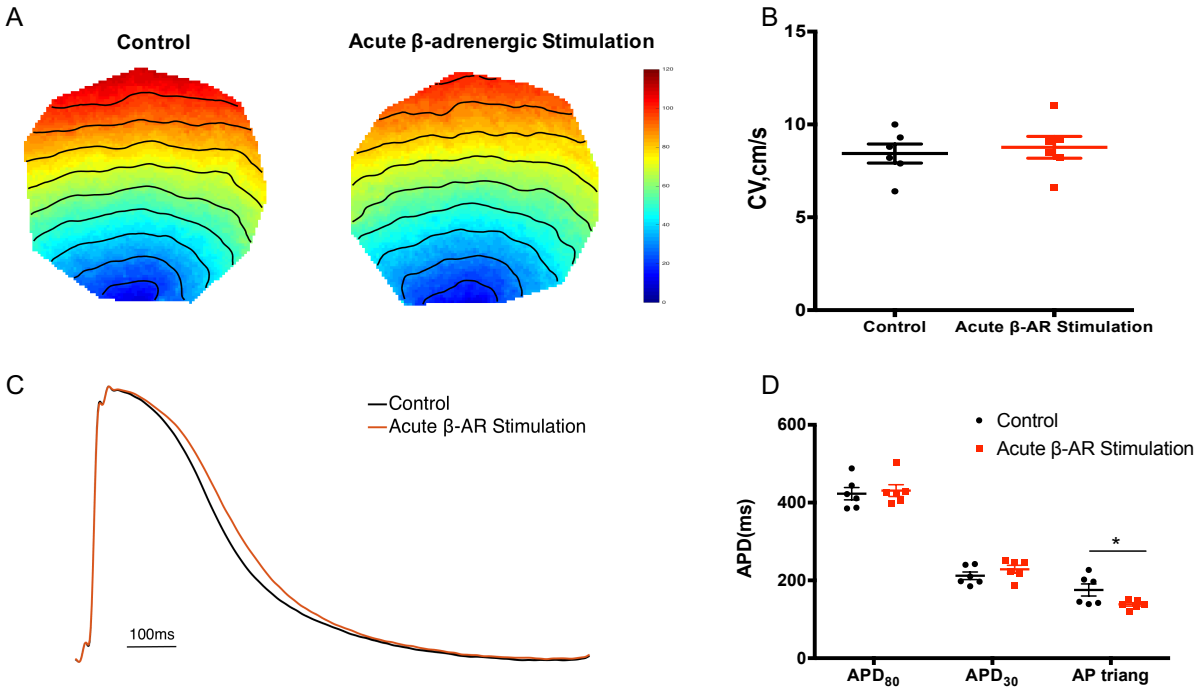

FIGURE 3

JPET Fast Forward. Published on March 26, 2020 as DOI: 10.1124/jpet.120.265686
This article has not been copyedited and formatted. The final version may differ from this version.

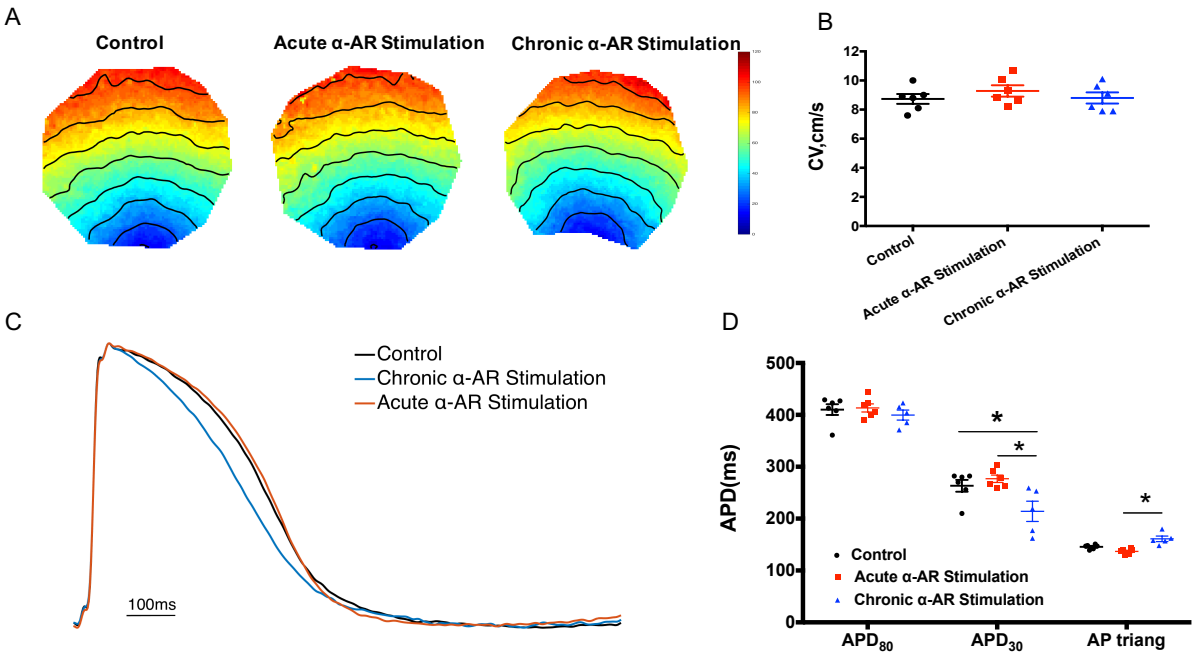

FIGURE 4

JPET Fast Forward. Published on March 26, 2020 as DOI: 10.1124/jpet.120.265686
This article has not been copyedited and formatted. The final version may differ from this version.

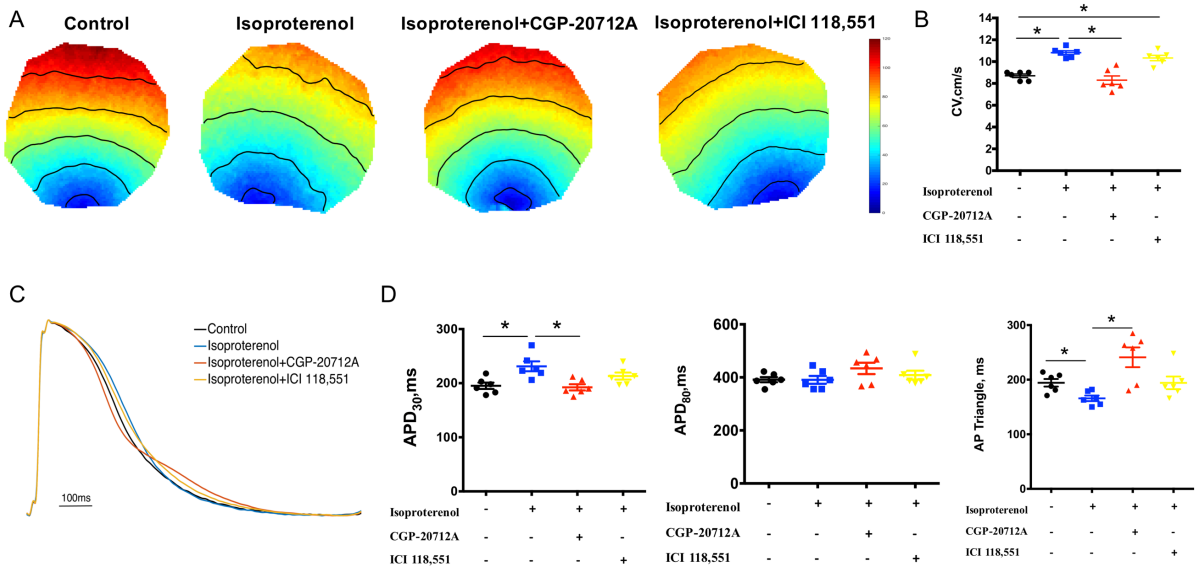

FIGURE 5

JPET Fast Forward. Published on March 26, 2020 as DOI: 10.1124/jpet.120.265686
This article has not been copyedited and formatted. The final version may differ from this version.

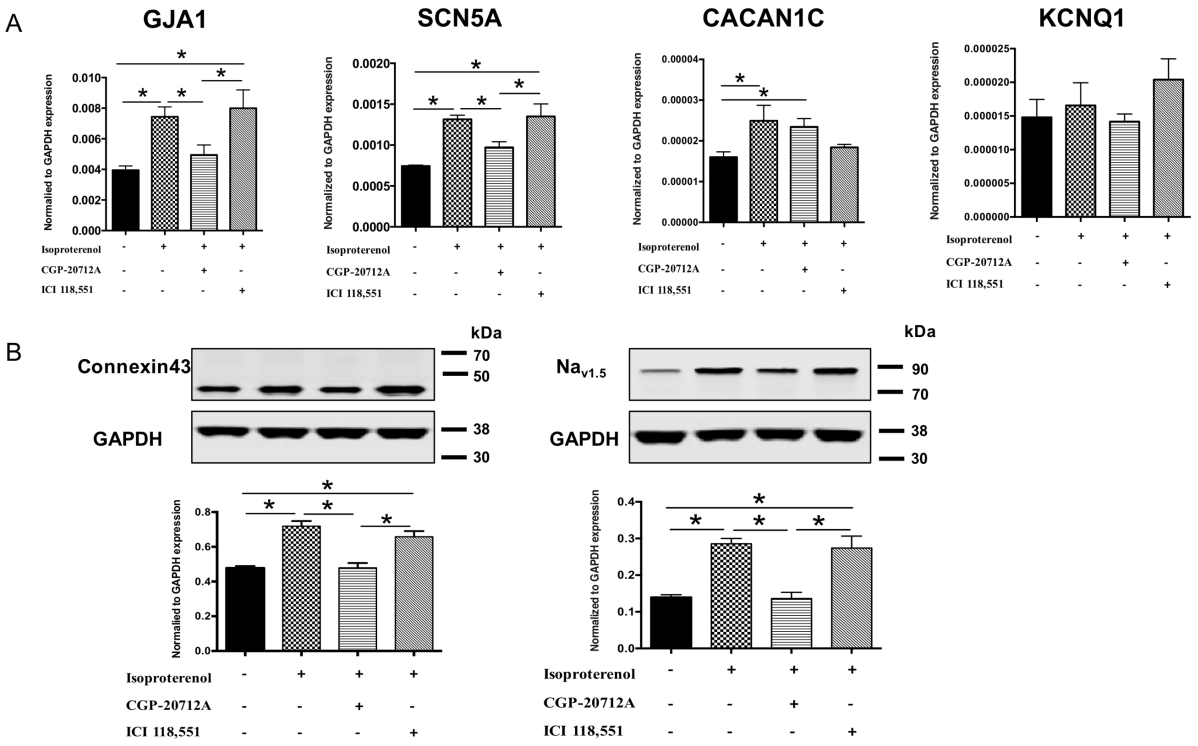

FIGURE 6

JPET Fast Forward. Published on March 26, 2020 as DOI: 10.1124/jpet.120.265686
This article has not been copyedited and formatted. The final version may differ from this version.

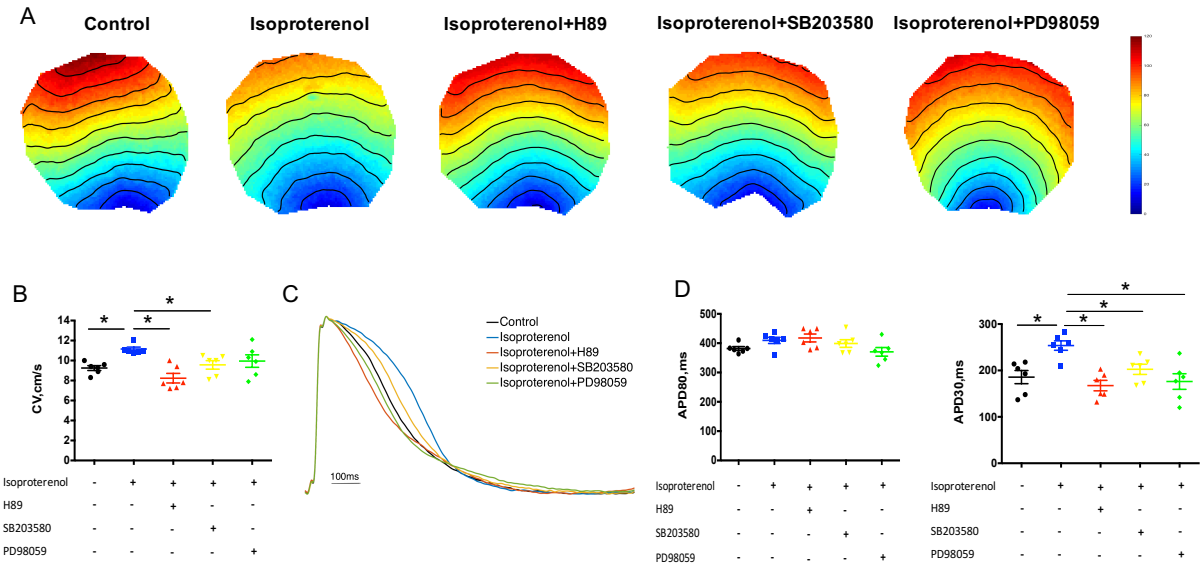

FIGURE 7

JPET Fast Forward. Published on March 26, 2020 as DOI: 10.1124/jpet.120.265686
This article has not been copyedited and formatted. The final version may differ from this version.

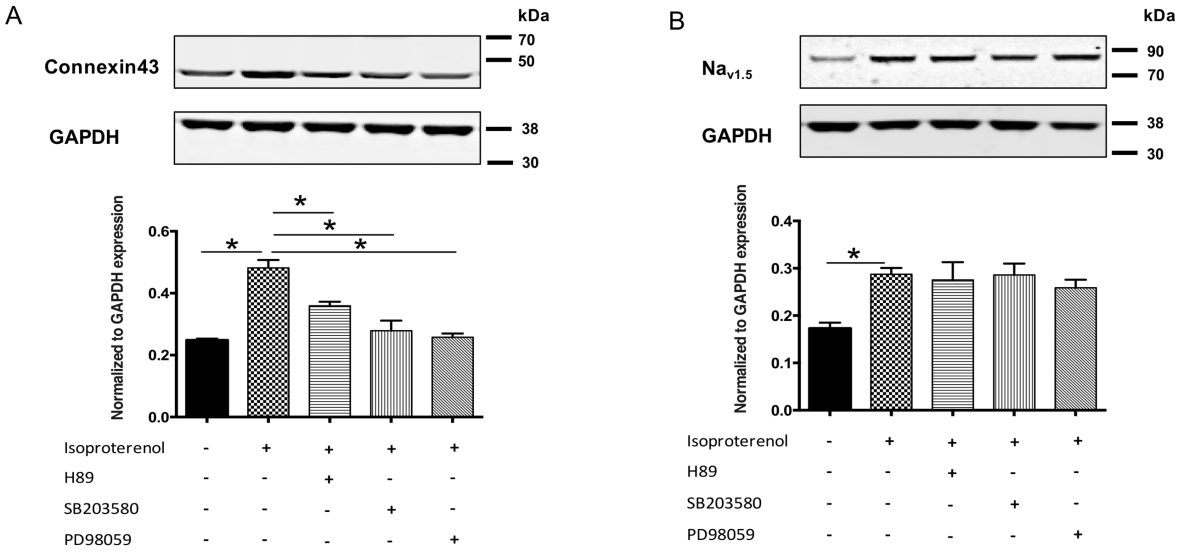

FIGURE8